Available online at www.sciencedirect.com
SCIENCE DIRECT
Surface Science 600 (2006) 2608–2613
SURFACE SCIENCE
www.elsevier.com/locate/susc

Investigating the lateral motion of SiGe islands by selective chemical etching

G. Katsaros [a,*], A. Rastelli [a], M. Stoffel [a], G. Isella [b], H. von Känel [b], A.M. Bittner [a], J. Tersoff [c], U. Denker [a], O.G. Schmidt [a], G. Costantini [a], K. Kern [a]

[a] Max-Planck-Institut für Festkörperforschung, Heisenbergstrasse 1, D-70569 Stuttgart, Germany
[b] L-NESS, Dipartimento di Fisica del Politecnico di Milano, Polo Regionale di Como, Via Anzani 52, I-22100, Como, Italy
[c] IBM Research Division, T.J. Watson Research Center, Yorktown Heights, New York 10598, USA

Received 18 August 2005; accepted for publication 21 April 2006
Available online 11 May 2006

Abstract

SiGe islands grown by deposition of 10 monolayers of Ge on Si(0 0 1) at 740 °C were investigated by using a combination of selective wet chemical etching and atomic force microscopy. The used etchant, a solution consisting of ammonium hydroxide and hydrogen peroxide, shows a high selectivity of Ge over Si_xGe_{1-x} and is characterized by relatively slow etching rates for Si-rich alloys. By performing successive etching experiments on the same sample area, we are able to gain a deeper insight into the lateral displacement the islands undergo during post growth annealing.

Keywords: Epitaxy; Etching; Atomic force microscopy; Surface structure; Morphology; Roughness and topography; Silicon; Germanium

Chemical etching processes have been used for a long time to characterize the structure of semiconductor materials. For example, they have been employed in the study of crystal symmetries, structural defects, etc. [1]. Nowadays, in combination with lithography-based techniques, they constitute a key step in the fabrication of semiconductor microdevices and microcomponents. The etching of semiconductors in liquid reactants is in fact widely used at all stages of the microsystem technology, such as for removing contaminants from the wafers, for creating three-dimensional structures, for revealing buried layers to define electrical contacts, etc.

More recently it has been shown that selective wet chemical etching combined with atomic force microscopy (AFM) measurements can also be used to obtain useful information about the composition of strained semiconductor islands [2–4]. These nanostructures, spontaneously formed during the initial stages of lattice mismatched semiconductor heteroepitaxy, have attracted the interest of many researchers since they are believed to offer a low-cost alternative for creating nanostructures on substrates compatible with the existing Si technology. Based on the selectivity of a hydrogen peroxide (H_2O_2) solution, that etches preferentially Ge over Si [2], it was possible to determine the spatial distribution of Si and Ge in nominally pure Ge pyramids, with a resolution of a few nanometers [3]. This was achieved by comparing the average morphology of the islands before and after etching. It was, however, not possible to follow the time evolution of the etching process since the Ge-rich parts of the islands are etched very fast.

In this paper we report a modification of the above used procedure. By combining selective wet chemical etching and AFM measurements, we are able not only to characterize the final etched structures, but also various intermediate etching stages of the *same island*. As an etchant we use a mixture consisting of ammonium hydroxide (NH_4OH), hydrogen peroxide (H_2O_2) and deionized water.

* Corresponding author.
E-mail address: g.katsaros@fkf.mpg.de (G. Katsaros).

0039-6028/$ - see front matter © 2006 Elsevier B.V. All rights reserved.
doi:10.1016/j.susc.2006.04.027

The same components, used at a different ratio and temperature, are widely used for removing several metal contaminants from the surface of silicon wafers and are known under the name RCA standard clean 1 (RCA SC1) [5]. We determine the etching rate of the solution for $Si_{1-x}Ge_x$ alloys as a function of Ge fraction x. By using this method we obtain new insights into (i) the origin of the Si incorporated into SiGe islands because of intermixing and (ii) the lateral island motion previously observed during post-growth annealing [6]. While Si–Ge intermixing occurring during growth and post-growth annealing has been extensively documented in the literature [3,4,7–11] the origin of the Si has been rarely discussed explicitly. Here we demonstrate that Si comes not only from the trenches surrounding the islands grown at relatively high temperatures, but mostly from the substrate regions right-below the wetting layer surrounding the islands. This results in an overall substrate lowering compared to the level prior to Ge growth [12]. While the intermixing occurs in a rather symmetric fashion during Ge deposition, post-growth annealing results in an asymmetric alloying and lateral island motion [6]. A discussion on the different mixing behavior during growth and annealing is presented.

The samples used for this study were grown by solid source molecular beam epitaxy. After chemical cleaning and deoxidation of the Si(001) wafer at 950 °C in ultra high vacuum, a 100 nm thick Si buffer was grown while ramping the substrate temperature from 480 °C to the island growth temperature of 740 °C. After a 5 s growth interruption, 10 monolayers (ML) of Ge were deposited at a rate of 0.04 ML/s and the samples were either directly cooled to room temperature at a rate of 1 °C/s, or kept at 740 °C for further 10 min before cooling. Prior to etching, $5 \times 5\ mm^2$ pieces were cut from the full 4 inch wafer and a cross-like mark was scratched on the surface in order to find more easily the same surface region after successive etching experiments. Fig. 1 is a micro-photograph of the sample showing the AFM cantilever positioned close to such a mark. The samples were dipped at room temperature in a 1:1 vol. (28% NH_4OH)/(31% H_2O_2) solution (VLSI Selectipur, Merck). After each etching experiment, they were rinsed in deionized water, the same sample position was located again and the morphology of the islands was investigated by means of AFM in tapping mode.

The dependence of the etching rate on the Ge content in Si_xGe_{1-x} alloys was determined by etching so-called virtual substrates [13]. They consisted of 1 μm thick strain-relaxed SiGe layers of different compositions on top of linearly graded SiGe buffers. The virtual substrates were grown by means of low energy plasma enhanced chemical vapor deposition [14]. Prior to their exposure to the etchant, some portions of the virtual substrates were masked with Apiezon wax W100, which acts like a resist. Such samples were then etched for a given time, after which they were rinsed with deionized water and the wax was removed with dichloromethane. The height difference between the masked and unmasked regions was determined by using a DEKTAK profilometer and the ratio of this height to the etching time was used as an evaluation of the etching rate. In order to obtain representative values, we repeated this procedure for different times and compositions. Fig. 2 shows the evolution of the etch rate with the Ge content in the Si_xGe_{1-x} alloy. While almost no etching effect is observed for a Ge content lower than 30%, the etching rate increases monotonically for higher Ge concentrations, demonstrating that this solution has a selectivity of Ge over $Si_{0.7}Ge_{0.3}$ of about 10^4.

The high selectivity is not easily explained. First, alkaline solutions, such as aqueous KOH, etch Si_xGe_{1-x} with concomitant hydrogen evolution; increasing Ge content decreases the etching rate [15]. Johnson et al. [16] showed that this is also true when aqueous NH_3 (NH_4OH) is used. In the presence of H_2O_2, the scenario changes, and Ge is predominantly dissolved (without hydrogen evolution). The reasons are on the one hand a fast passivation of the Si by the Si oxide produced from Si and H_2O_2, on the other hand the strongly increased etching (oxidation) rate of Ge, which does not form passive layers. The mechanism proposed by Johnson et al. [16] should be valid for bulk samples of either pure Si or pure Ge. Note that the

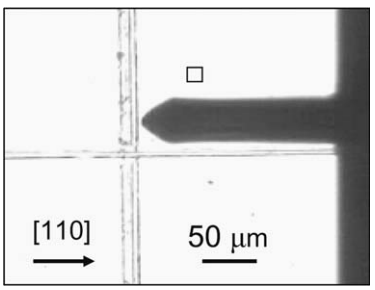

Fig. 1. Micro-photograph (magnification factor 180) showing the positioning of the AFM cantilever at the corner of the mark on the sample surface. This allows the measurement of the same surface area after every etching experiment. The square area shown close to the cantilever corresponds to the maximum scan range of the AFM ($13.4 \times 13.4\ \mu m^2$).

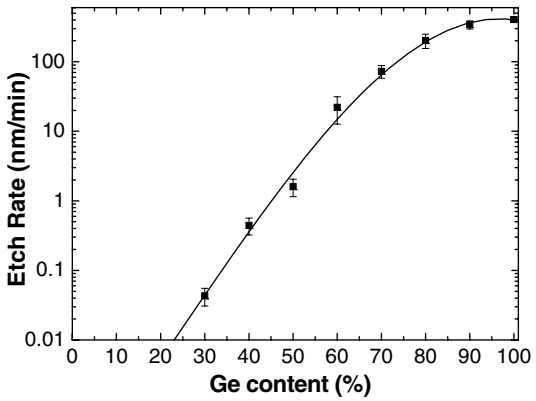

Fig. 2. Etching rate of a 1:1 (28% NH_4OH)/(31% H_2O_2) solution as a function of the Ge concentration determined on Si_xGe_{1-x} virtual substrates.

chemical reactivity may be altered on the nanoscale, i.e. surfaces of very small lateral extension cannot be expected to show the same behaviour. However, our observations are in line with the mechanism proposed by Johnson et al. (etching rate increases with increasing Ge content).

We cannot determine whether our SiGe islands and virtual samples show complete intermixing on the atomic scale, or whether nanoscale volumes of relatively pure Si (or Ge) are present [17–19]. In the latter case, the reactivity would only differ slightly from that of the pure elements (passivation of Si and dissolution of Ge). In contrast, Si–Ge bonds, rather than Si–Si or Ge–Ge bonds, would dominate the chemical behavior for intermixing – in this case our observations are quite surprising, since the chemical reactivity should be different from that of the elements.

Fig. 3 shows AFM images of the same surface region for the as-grown [left column (a)–(c)] and annealed islands [right column (d)–(f)] at different etching times. The as-grown sample consists of a monomodal distribution of barns [20,21]; they are etched in an almost symmetric way as can be seen in Fig. 3(b). After complete removal of the islands, circular plateaus can be observed below each island [Fig. 3(c)]. The annealed sample, on the other hand, shows pyramids and transition islands (i.e., islands intermediate between pyramids and domes) [22–24]. It is interesting to note that all islands on this sample are asymmetrically etched. In particular, the steepest parts of the islands are first attacked by the etchant [see arrows in Fig. 3(d) and (e)]. After the complete removal of the islands, half-moon-like structures become visible, having a diameter comparable to that of the circular plateaus observed in the as-grown samples [Fig. 3(f)]. Also the morphology of the trenches surrounding the islands differs significantly after in-situ annealing. While they are almost square shaped with sides aligned along the ⟨100⟩ directions for the as-grown sample [12] [Fig. 3(c)], upon annealing they become much more irregular and deeper and wider on one side [darker areas next to the 'half-moons' seen in Fig. 3(f)].

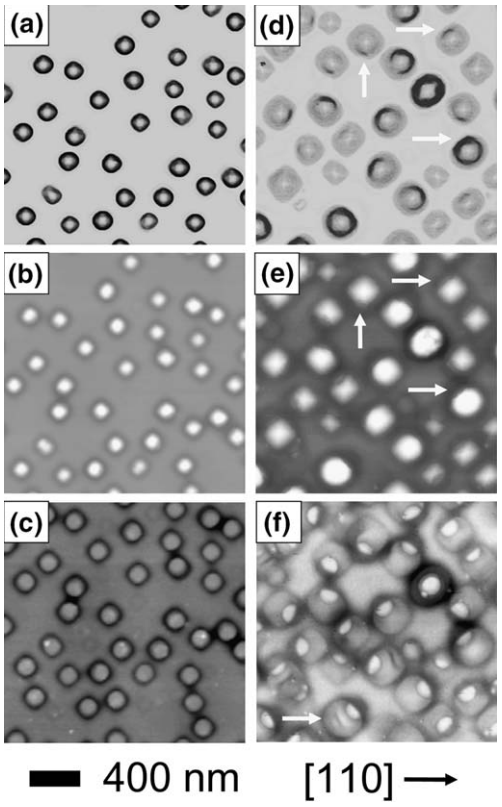

Fig. 3. AFM images showing as-grown (left column) and annealed islands (right column) before and after different etching times. In both cases the same region was imaged after successive etching experiments. In (a)–(c) the as-grown islands are shown after 0, 40 and 150 min of etching, respectively. (d)–(f) show the annealed islands after 0, 80 and 620 min of etching, respectively. For the images of the non-etched samples [(a) and (d)] the grayscale is related to the local surface slope so that steep (darker) and shallow (brighter) facets can be distinguished. For the remaining images the grayscale represents the local surface height and is separately adjusted in order to get the highest contrast. For the annealed islands the etching is always asymmetric and starts at the steeper facets as indicated by the arrows in (d) and (e). The arrow in (f) shows a secondary trench, probably created by a temporary interruption in the island movement (see text).

The circular plateaus observed in Fig. 3(c) are interpreted as the original interface between the islands and the Si substrate. By measuring their height, we determined that they lie on average 1.1 nm higher than the surrounding surface. This could be the result of an overall lowering of the substrate surface [12], taking place during growth (Fig. 4). In order to support this hypothesis, we first note that the as-grown islands shown in Fig. 3(a) are highly intermixed. Indeed, their total volume per unit area corresponds to about 2.9 nm as determined by AFM, while the deposited 10 ML of Ge are only equivalent to 1.4 nm. This indicates an average Si composition higher than 50%, consistently with anomalous X-ray scattering measurements performed on similar samples [11]. The trenches surrounding the islands cannot be the only source of Si, since their volume amounts only to 0.3 nm. Since at the temperatures used (740 °C) bulk diffusion is not significant [6], the extra 1.2 nm of Si material must necessarily come from the substrate regions located in between the islands. On the other hand, if Si reaches the islands by surface diffusion after having moved through a thin and intermixed wetting layer, a uniform substrate lowering would occur except for in the regions below the islands [Fig. 4(b)–(d)]. This is exactly what we observe in the etched sample in Fig. 3(c), and the measured height difference of 1.1 nm between the plateaus and the surrounding substrate is in good agreement with the value of the "missing" Si evaluated above.

A further experimental support to this interpretation derives from exposing an as-grown sample to the etching solution for 1700 min. The etching rates reported in Fig. 2 were measured for Si contents up to 70%, since for higher concentrations the etching time required to obtain a height difference observable with the profilometer becomes very long and the height measurements unreliable.

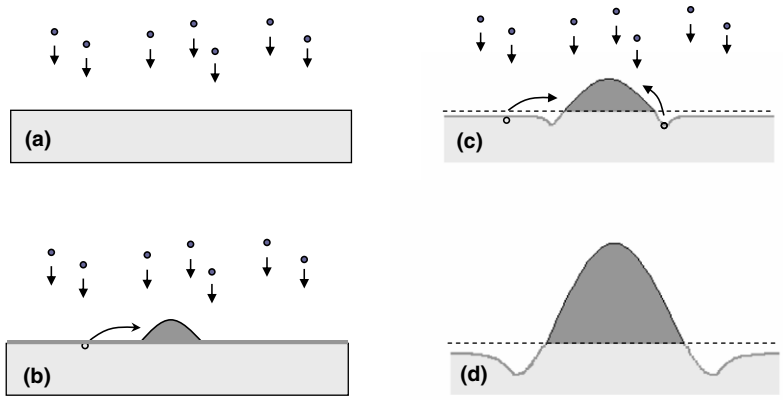

Fig. 4. Schematic representation of the lowering of the substrate level during growth. (a) Ge atoms are deposited on Si. (b) Islands grown from Ge atoms and Si diffusing through the WL. (c) Islands continue to grow and induce an out diffusion of the surrounding highly strained material that produces a trench. In this way Si-rich material from the trenches gets incorporated into the islands. Due to the incorporation of substrate Si atoms, the lowering of the WL level has already started. (d) Final situation with the island surrounded by its trench and its interface lying higher than the surrounding surface.

Nevertheless, by extrapolation, we can evaluate an etching rate of about 1 pm/min for a $Si_{0.9}Ge_{0.1}$ alloy. Thus, if the composition of the plateaus was of $Si_{0.9}Ge_{0.1}$, their height should be reduced by more than 1 nm after 1700 min of etching. On the contrary, the plateaus remained almost unchanged, indicating that they consist of at least 90% Si. This experiment further demonstrates that strain-driven bulk interdiffusion, even if present, modifies only slightly the original interface between the island and the substrate.

A quantitative comparison of the AFM images for as-grown [Fig. 3(a)] and annealed samples [Fig. 3(d)] reveals that the island density decreases from 8.8 to 6.7 μm^{-2} and that the total island volume increases from 2.9 to 3.2 nm. This implies that the post-growth annealing induces an island coarsening accompanied by a further incorporation of Si within the islands [7,25]. The latter statement is further supported by the observation that, after 70 min of etching, two times more material has been removed from the as-grown sample with respect to the annealed ones. The anisotropic etching observed in Fig. 3(e), as well as the peculiar half-moon plateaus visible in Fig. 3(f) indicate a rather complex SiGe material distribution within the annealed islands. In order to understand its microscopic origin, we examined the island erosion at different etching stages by focusing on particular islands and taking line scans after various etching times. As a reference, the left column in Fig. 5 shows the 'time-resolved' etching of a typical as-grown island. The material is removed almost symmetrically and finally the circular plateau buried below the island is revealed (Fig. 5(d)). Conversely, both dome (middle column) and pyramid-like (right column) annealed islands are etched quicker from one side. In particular, this is the steeper side of the island, below which the half-moon like structure can be found. Based on the selectivity of the etchant, we conclude that this part of the island is Ge-richer. Fig. 5(h) and (l) clearly show the morphology of the trenches surrounding the annealed islands, which actually consist of two distinct regions. The first is smaller and deeper and surrounds only the half-moon, while the second is shallower and larger and completely encircles the island. The evolution of the island etching is summarized by the AFM line-scans taken at the different stages of the etching process [Fig. 5(m)–(o)].

We interpret the above observations as a consequence of a lateral motion of the islands [6]. Islands close to each other have a high strain energy density in the region between them. It has been recently shown that under these conditions, material tends to migrate away from the region located in between two neighboring islands [26]. This provides the trigger for a self-sustaining process in which material leaves one side of the island, mixes with Si from the substrate, and redeposits on the opposite side [6]. A more dilute SiGe alloy is thus formed on the side pointing away from adjacent neighbors. After the initial trigger, the driving force for the self-sustaining motion is the reduction in free energy as material from the island intermixes with Si from the substrate. Because bulk diffusion is negligible, such mixing cannot readily occur without island motion. Consequently, while the islands are growing during the post-growth annealing, their center of mass is moving because of the internal redistribution of Ge and the asymmetric incorporation of Si (see Fig. 6).

During the lateral island displacement, part of their interface with the original Si substrate is exposed. The atoms belonging to this region are under compressive strain generated by the receding islands' edges and thus diffuse away as they are uncovered [Fig. 6(b)]. As a result, a wide and deep trench is created on this side of the islands, while the portion of the interface that is still covered remains unchanged. This explains why, when the islands of the annealed sample are completely removed by etching, instead of full plateaus only fractions of them – the above mentioned "half-moons" – appear [Fig. 3(f)].

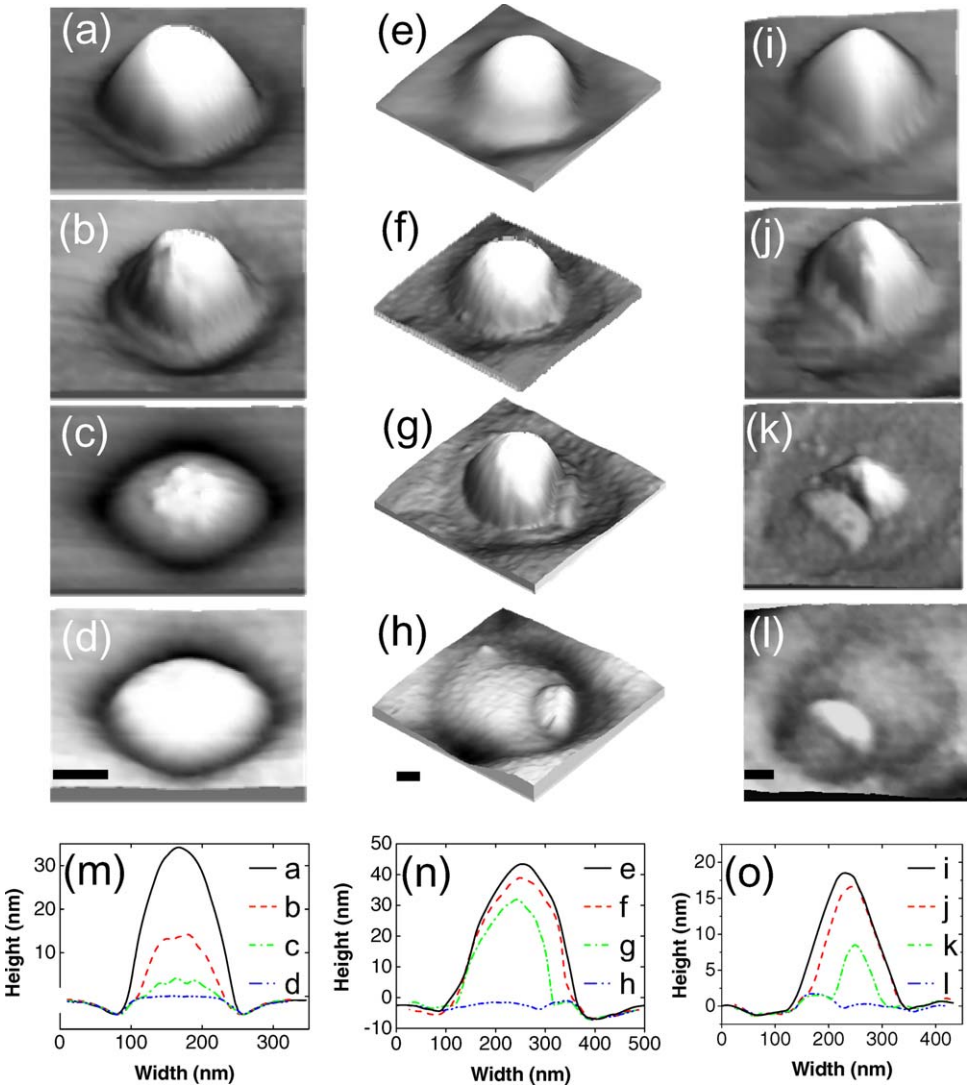

Fig. 5. AFM topographies showing successive stages of the etching of three different islands. (a)–(d) for an as-grown island, (e)–(h) for an annealed dome and (i)–(l) for an annealed pyramid-like island. The corresponding linescans (m)–(o) demonstrate that, while the as-grown island is etched isotropically, the annealed islands are etched quicker from their steeper side, below which the half-moon shaped plateaus are finally emerging. The scale bars correspond in each case to 50 nm. The time intervals are 0, 40, 60 and 150 min for (a)–(d) while for (e)–(h) and (i)–(l) they are 0, 80, 170 and 620 min respectively.

The advancing part of the islands, as discussed above, is highly intermixed and less strained and therefore favors a shallower surface orientation [7,27,28]. Thus, the annealed islands exhibit an asymmetric shape [Fig. 3(d)]. The trenches formed around the relaxed parts of the islands are shallower and are constantly overgrown because of the island movement. It appears that in some cases this movement is interrupted for some time so that a deeper trench is formed between the initial and the final one as can be sometimes observed in the etched samples [see arrow in Fig. 3(f)]. We see that the above reported complex mechanism, schematically shown in Fig. 6, fits quite well with all the experimentally observed features. Actually, also for samples grown and annealed at lower temperatures (620 °C) a similar mechanism can explain the experimentally observed complex composition profiles of the dome islands [4].

Our interpretation [6] is further supported by the observation that the as-grown islands grown at 740 °C do not show any sign of a lateral motion, even though also on the as-grown sample there are islands very close to each other [Fig. 3(c)], i.e. the strain field needed to trigger the motion is present. The reason for this is that the strain field is just the trigger; the real driving force for the motion is the intermixing of the Ge-rich island with Si from the substrate, which during annealing cannot readily occur except by island motion.

This driving force is reduced or eliminated during growth. Material is continually depositing on all sides of the island; but mixing of island material with Si from the substrate occurs only if there is net removal of material from one side. Even if the island can maintain a net removal of material from one side, the benefit is largely lost during growth. During annealing, the only source of

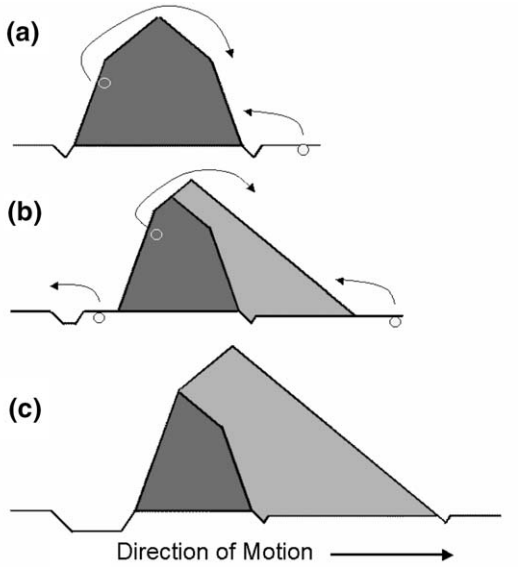

Fig. 6. Schematic representation of the lateral island movement during annealing. (a) Ge rich material (dark gray) is diffusing from one side of the island to the opposite one, where it intermixes with Si atoms (light gray) originating from the substrate, and creates a SiGe alloy (gray). (b) The part of the Si plateau, which is uncovered diffuses away. (c) The final island has a deeper and wider trench on the Ge rich side (remnant of the initial island) and a shallower trench surrounding its newly grown part.

material is the Si substrate, so the source has very different composition than the island, and mixing lowers the free energy. However, during continuous growth some mixing can occur between the flux and the substrate even before the material diffuses to the island and incorporates. And the continuous nature of the process means that the material arriving at the island generally has the same composition as the island itself, so lateral motion does not drive further compositional mixing in the same way as during annealing.

In conclusion, we have investigated the lateral SiGe island motion occurring during post growth annealing by applying selective wet chemical etching. By analyzing the different etching stages on the same island, detailed information on the island composition can be obtained. While an almost symmetric composition profile is observed for as-grown islands, we give evidence of an asymmetric composition profile in annealed islands, demonstrating thus that chemical etching based methods are a powerful tool to investigate the formation and evolution of semiconductor nanostructures. By using the etching curve presented in Fig. 2 and by etching the same sample area several times it is possible, in principle, to build-up a complete compositional map of each island. This would allow our technique to directly access the composition profiles of individual islands with unprecedented statistics and high resolution.

References

[1] K. Sangwal, Etching of Crystals, North-Holland, Amsterdam, 1987.
[2] O.G. Schmidt, U. Denker, S. Christiansen, F. Ernst, Appl. Phys. Lett. 81 (2002) 2614.
[3] U. Denker, M. Stoffel, O.G. Schmidt, Phys. Rev. Lett. 90 (2003) 196102.
[4] G. Katsaros, G. Costantini, M. Stoffel, R. Esteban, A.M. Bittner, A. Rastelli, U. Denker, O.G. Schmidt, K. Kern, Phys. Rev. B 72 (2005) 195320.
[5] W. Kern, Handbook of Semiconductor Wafer Cleaning Technology, Noyes Publications, Park Ridge, NJ, 1993.
[6] U. Denker, A. Rastelli, M. Stoffel, J. Tersoff, G. Katsaros, G. Costantini, K. Kern, N.Y. Jin-Phillipp, D.E. Jesson, O.G. Schmidt, Phys. Rev. Lett. 94 (2005) 216103.
[7] T.I. Kamins, G. Medeiros-Ribeiro, D.A.A. Ohlberg, R.S. Williams, Appl. Phys. A 67 (1998) 727.
[8] S.A. Chaparro, J. Drucker, Y. Zhang, D. Chandrasekhar, M.R. McCartney, D.J. Smith, Phys. Rev. Lett. 83 (1999) 1199.
[9] F. Boscherini, G. Capellini, L. Di Gaspare, F. Rosei, N. Motta, S. Mobilio, Appl. Phys. Lett. 76 (2000) 682.
[10] A. Malachias, S. Kycia, G. Medeiros-Ribeiro, R. Magalhães-Paniago, T.I. Kamins, R.S. Williams, Phys. Rev. Lett. 91 (2003) 176101.
[11] T.U. Schülli, M. Stoffel, A. Hesse, J. Stangl, R.T. Lechner, E. Wintersberger, M. Sztucki, T.H. Metzger, O.G. Schmidt, G. Bauer, Phys. Rev. B 71 (2005) 035326.
[12] U. Denker, O.G. Schmidt, N.Y. Jin-Phillipp, K. Eberl, Appl. Phys. Lett. 78 (2001) 3723.
[13] E.A. Fitzgerald, Y.-H. Xie, M.L. Green, D. Brasen, A.R. Kortan, J. Michel, Y.-J. Mii, B.E. Weir, Appl. Phys. Lett. 59 (1991) 811.
[14] G. Isella, D. Chrastina, B. Rößner, T. Hackbarth, H. Herzog, U. König, H. von Känel, Solid-state Electron. 48 (2004) 1317.
[15] E. Fitzgerald, K.C. Wu, M. Currie, N. Gerrish, D. Bruce, J. Borenstein, Mat. Res. Soc. Symp. Proc. 518 (1998) 233.
[16] F.S. Johnson, D.S. Miles, D.T. Grider, J.J. Wortman, J. Electron. Mat. 21 (1992) 805.
[17] E. Müller, H.-U. Nissen, M. Ospelt, H. von Känel, Phys. Rev. Lett. 63 (1989) 1819.
[18] P. Venezuela, J. Tersoff, J.A. Floro, E. Chason, D.M. Follstaedt, F. Liu, M. Lagally, Nature 397 (1999) 678.
[19] A. Malachias, T.U. Schülli, G. Medeiros-Ribeiro, L.G. Cançado, M. Stoffel, O.G. Schmidt, T.H. Metzger, R. Magalhães-Paniago, Phys. Rev. B 72 (2005) 165315.
[20] E. Sutter, P. Sutter, J.E. Bernard, Appl. Phys. Lett. 84 (2004) 2262.
[21] M. Stoffel, A. Rastelli, T. Merdzhanova, O.G. Schmidt, submitted for publication.
[22] G. Medeiros-Ribeiro, A.M. Bratkovski, T.I. Kamins, D.A.A. Ohlberg, R.S. Williams, Science 279 (1998) 353.
[23] F.M. Ross, R.M. Tromp, M.C. Reuter, Science 286 (1999) 1931.
[24] F. Montalenti, P. Raiteri, D.B. Migas, H. von Känel, A. Rastelli, C. Manzano, G. Costantini, U. Denker, O.G. Schmidt, K. Kern, L. Miglio, Phys. Rev. Lett. 93 (2004) 216102.
[25] T.I. Kamins, G. Medeiros-Ribeiro, D.A.A. Ohlberg, R.S. Williams, J. Appl. Phys. 85 (1999) 1159.
[26] M. Stoffel, A. Rastelli, S. Kiravittaya, O.G. Schmidt, Phys. Rev. B 72 (2005) 205411.
[27] A. Rastelli, M. Kummer, H. von Känel, Phys. Rev. Lett. 87 (2001) 256101.
[28] W.L. Henstrom, C.-P. Liu, J.M. Gibson, T.I. Kamins, R.S. Williams, Appl. Phys. Lett. 77 (2000) 1623.